22π-electrons [1.1.1.1.1] pentaphyrin as a new photosensitizing agent for water disinfection: Experimental and Theoretical characterization

Marta E. Alberto,[a] Clara Comuzzi,[b] Merlyn Thandu[b], Carlo Adamo,[a] Nino Russo[c]*

[a] *Institut de Recherche de Chimie Paris, IRCP CNRS UMR-8247, École Nationale Superieure de Chimie de Paris, Chimie ParisTech, 11 rue P. et M. Curie, 75005 Paris, France*

E-mail: marta.alberto@chimie-paristech.fr

[b] *Department of Chemistry, Physic and Environment, University of Udine, Via del Cotonificio 108, 33100 Udine, Italy*

[c]*Dipartimento di Chimica e Tecnologie Chimiche, Università della Calabria, Via P. Bucci, 87036 Rende, Italy;*

KEYWORDS: ROS, TDDFT, $^1O_2$

D*edicated to the UNESCO International Year of Light and Light-based Technologies (IYL 2015)*

ABSTRACT

In view of their promising photosensitizing features, expanded porphyrins are gaining wide attention for their potential use in both photodynamic therapy (PDT) of cancer or as likely photoactivated agent for water disinfection. Herein, we report a joint experimental and theoretical investigation on the 20-(4'-carboxyphenyl)-2,13-dimethyl-3,12-diethyl-[22]pentaphyrin complex **4**. The synthesis, NMR, UV-Vis and mass characterization of the new

compound together with a detailed theoretical investigation of the photophysical properties are presented. In particular, type I- and type II- photoreactions have been explored by means of DFT and its TDDFT formulation characterizing the electronic absorption spectra, providing singlet-triplet energy gap, vertical ionization potential and electron affinity. Results show that title compound is able to generate the cytotoxic singlet oxygen species supporting the application of the proposed molecule as a photoactivated agent for water disinfection.

1. Introduction

Expanded porphyrins are porphyrogenic macrocycles where five or more pyrroles are linked together mainly through direct α, α connections or CH= bridges. In the past decades many macrocycles have been synthesized and characterized allowing a better understanding of fundamental concepts as aromaticity, π conjugation, structural dependence and discovering new physical and chemical features expanding the potential application of these molecules. [1,2] The plethora of fields in which they can be applied spans from biomedical, to cation or anion binding application and lately near infrared materials. [3-7] Recently, several expanded porphyrins have been synthesized and characterized in view of their promising photosensitizing features [8-10]. The so-called photodynamic effect rests in the oxidative damage of biological material by reactive forms of oxygen generated by sensitized reactions. The photodynamically active species is singlet oxygen $^1O_2$ generated in situ by energy transfer from an excited sensitizer to oxygen molecule. The photodynamic effect is being utilized in several fields [11], e.g., photodynamic therapy (PDT) [12-15] of cancer or atherosclerosis, inactivation of some bacteria and viruses and insecticides [16-19]. In the photodynamic therapy of tumors, a photosensitizing agent (PS) is injected intravenously and it is excited from its electronic ground state (S_0) to the

first excited state (S_1) by using light of a specific intensity. The exited triplet state generated through radiationless intersystem crossing transition, in oxygenated environments and under certain conditions, can transfer its energy to ground-state molecular oxygen ($^3O_2$) generating the cytotoxic singlet oxygen ($^1O_2$) (type-II photoreactions). On the other hand, the excited PS can react directly with organic substrates by electron exchange producing radical intermediates that are subsequently scavenged by oxygen, with the formation of the superoxide oxygen radical species $O_2^{\cdot(-)}$ and other highly reactive radicals (ROS). (Type-I photoreactions) [11-15]

Beside the well-known application as useful pro-drugs for the treatment of some cancers and diseases, the oxidant conditions generated by the irradiation of the photosensitizer can be exploited also in environmental application. As a consequence, photochemical remediation approaches, exploiting the oxidizing capacity of ROS, have significant application for water treatment and disinfection processes. [16] Actually, it is well recognized that photochemically generated $^1O_2$ acts as a primary oxidant in the photosensitized transformation of organic substances [17] and inactivation of viruses [18-19] in natural waters. Porphyrins are highly effective for $^1O_2$ production in response to visible light, and among various photoactive generating agents, some of them have been already employed for the oxidative degradation of various contaminants and for bacterial/viral disinfection in water [20-21].

Members of [1.1.1.1.1] pentaphyrins, a class of expanded porphyrins made of five pyrrolic rings linked by *meso*-like bridges, have been proposed for their use in PDT. In particular, the non-aromatic (reduced form) 24 π-electrons iso-pentaphyrins (**1**) and the aromatic (oxidized form) 22 π-electrons pentaphyrin (**2**), have been synthesized, characterized and tested [22-23] as photosensitizing agents (Scheme 1). Both compounds have been found to cause cell death by apoptosis, although the aromatic pentaphyrin **2** appeared to be a more efficient photosensitizer

than the nonaromatic analogues macrocycle **1**. A slightly modified non-aromatic iso-pentaphyrin**,** obtained replacing the diethyl-pyrrole with an unsubstituted pyrrole and by introducing a carboxylic group on the phenyl substituent (**3**), and its lutetium(III) complexes has been reported and also tested for potential application in PDT. [24] Both compounds were found not able to produce singlet oxygen by irradiation, from both experimental and theoretical point of views. [24-25]

Herein we report a joint experimental and theoretical investigation of the new 20-(4'-carboxyphenyl)-2,13-dimethyl-3,12-diethyl- [22] pentaphyrin complex **PCCox** (**4).** The photoactivation properties of the novel expanded porphyrin were recently tested in water disinfection, using S. Aureus as a Gram-positive bacteria model and data showed that **4** was effective against these bacteria at nanomolar concentration [26-27]. A detailed theoretical investigation of the photophysical properties of the proposed molecule is herein presented, together with the synthesis, NMR, UV-Vis and mass characterization of the new compound. Type I and type II photosensitized processes have been explored at DFT and its TDDFT [28] formulation. These methods have been previously and successfully employed to explain the structural and spectroscopic features of a large series of systems including different type of photosensitizers active in PDT [25,29-35].

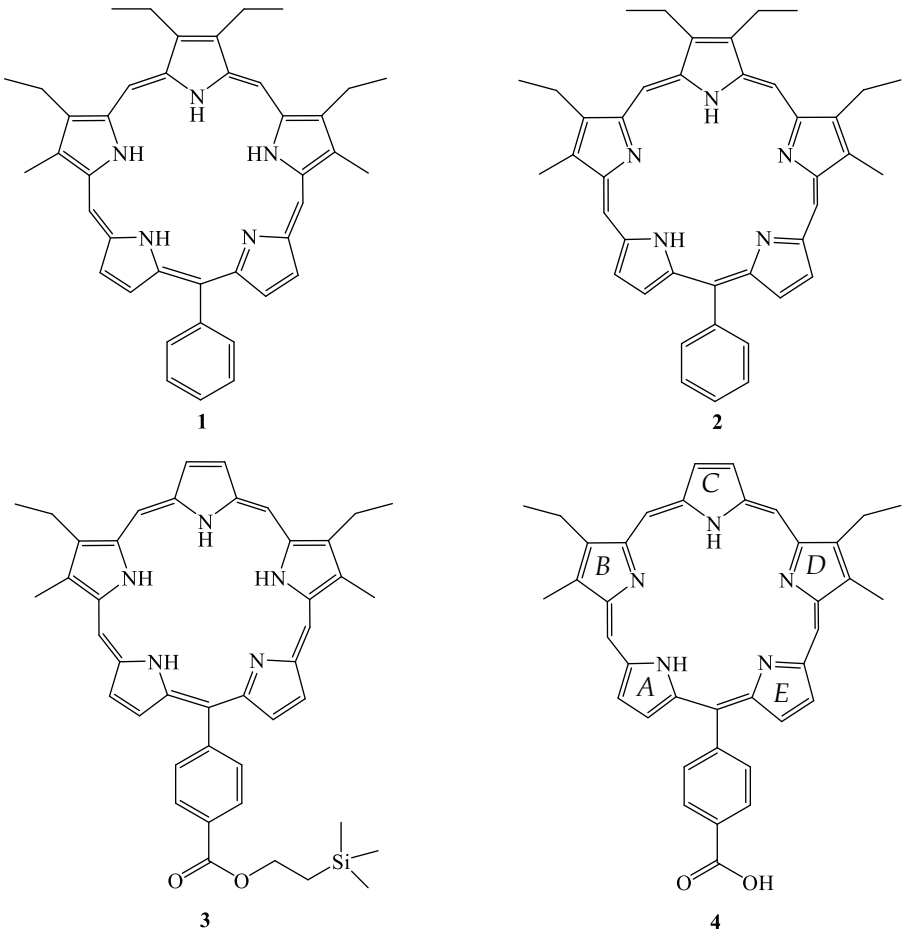

Scheme 1. Structures of 24 π-electrons iso-pentaphyrins (**1**), aromatic 22 π-electrons pentaphyrin (**2**), modified iso-pentaphyrins (**3**) and the herein investigated 20-(4'-carboxyphenyl)-2,13-dimethyl-3,12-diethyl- [22] pentaphyrin **PCCox (4)**

2. Results and Discussion

2.1 Synthesis and Characterization of PCCox

PCCox 4 was obtained by oxidation in air of a solution of the reduced form **3** [24] (in CH_2Cl_2 / TFA 1: 1); the reaction was quantitative in 48 h. In this step the deprotection of the carboxyl function was also achieved.

The ESI-MS (positive mode, Acetonitrile) showed the molecular ion peak at m/z 592 ($[MH]^+$) (See Supplementary Material). The ESI-MS^2 fragmentation pattern of the $[M + H]^+$ ion of the

PCCox (m/z 592) showed two intense radical ions at m/z 577 and 563 corresponding to the loss of CH_3 and C_2H_5 radicals, respectively, and two much less intense ions at m/z 483 and 471 due to the neutral displacing of one of the two dialkylated pyrrole moiety ($C_7H_{11}N$) and the benzoic acid radical ($C_7H_5O_2$), respectively. These experiments show that the stability of the skeleton of **PCCox** is probably tied to its aromaticity (22-π electrons).

The ^{1}H NMR of PCCox as free base recorded in CD_3OD and $CDCl_3$ could not be resolved due to excessive line broadening. As already described for other pentaphyrins [23] also **PCCox** seems to be a flexible macrocycle which can adopt several conformations in solution most of which distorted. TFA addition to a PCCox solution in $CDCl_3$ allowed the characterization of the molecule. The ^{1}H NMR spectrum in $CDCl_3$ containing 33% of trifluoroacetic acid (TFA) shows the typical resonances of an aromatic pentaphyrin (Figure 1).

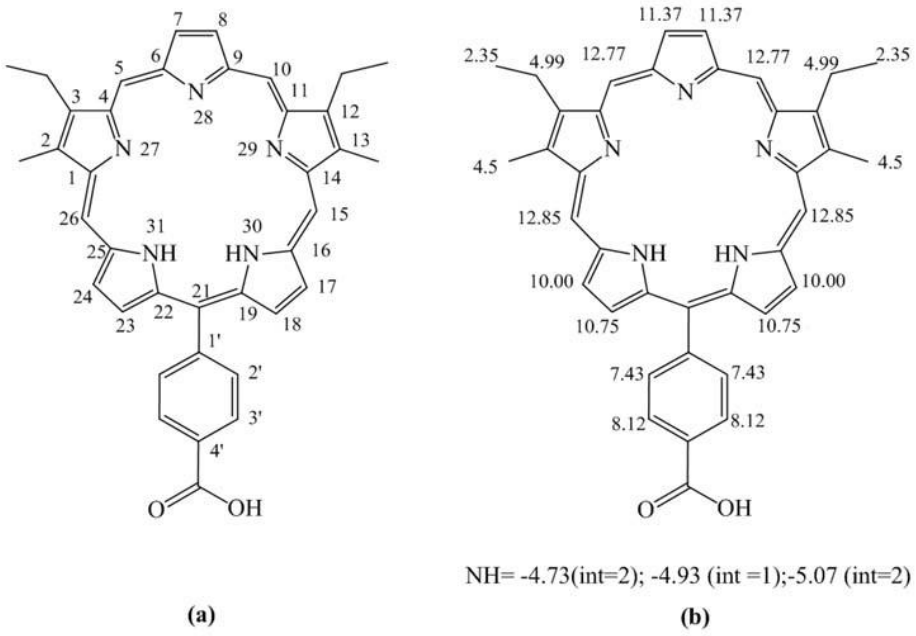

Figure 1. (a) Structure of 20-(4'-carboxyphenyl)-2,13-dimethyl-3,12-diethyl-[22] pentaphyrin **PCCox** with numbering; (b) ^{1}H-NMR chemical shift values in $CDCl_3$ containing 33% (v/v) TFA.

In fact, all the signals of the molecule undergo a shift due to the ring current effect. The NHs experience a huge upfield shift appearing at δ -4.73, -4.93 and -5.07 ppm (in a 2:1:2 ratio). These data demonstrate that in the experimental conditions ($CDCl_3$ containing 33% of trifluoroacetic acid (TFA)) PCCox is fully protonated and all the pyrroles are pointing inwards. The signals belonging to the alkylic chains in the periphery of the macrocycle are all shifted downfield as well as the β-pyrrolic protons (δ values at 11.37, 10.75 and 10 ppm) and the *meso*-CH (δ values at 12.85 and 12.77 ppm). This severe downfield shifting demonstrated that in PCCox (in CDCl3 33% TFA) none of the unsubstituted pyrrole or the meso-CH is flipped inside the ring. All the assignements were confirmed by 2D NMR experiments (COSY and NOESY) and are in agreement with other aromatic pentaphyrins already described [22-23].

The ^{1}H NMR of **PCCox** in neat TFA-*d* shows the appearance of signals between 1 and 0 ppm. Unfortunately, the spectrum was too complicated to be interpreted, but literature data suggest that strong acidic condition favors conformations with meso and/or pyrrolic protons flipped inside the ring where the aromatic current shifts the signals upfield. [1] It has to be stressed that mass and spectrophotometric analysis show no decomposition of **PCCox** upon any of the acidic treatments. Therefore, the severe signal shifts are to be ascribed only to conformational changes.

The absorption spectra of a solution of **PCCox** 1.24 x 10^{-4} M in methanol together with the spectrum of the same solution added with 200μl of TFA (the spectrum was not changing with time). The free base spectrum shows the Soret-like band of the free base at 462 nm (logε = 3.18) together with two bands in the UV region (370 and 320 nm) and a NIR band at 792 nm, (logε = 2.7). The addition of 200 microliters of TFA to this solution caused the appearance of a new band at 617 nm (log ε =2.5), the shift of the Soret band at 480nm while the NIR band remained unchanged.

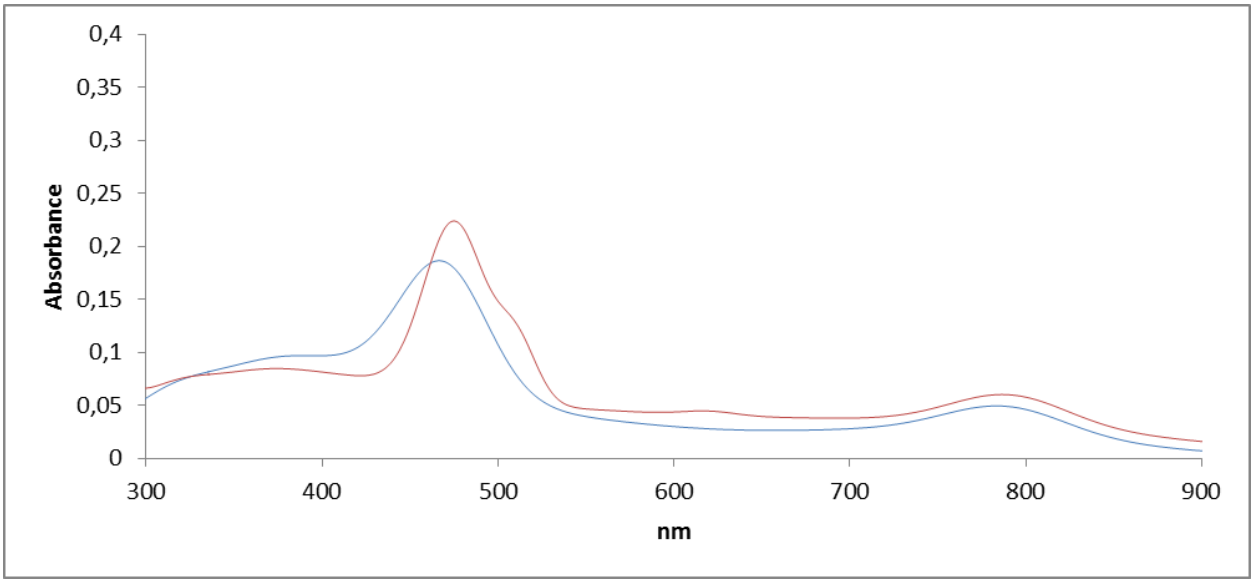

Figure 2. Absorption UV-vis spectra of PCCox **4** 1.24 x 10^{-4} M in CH_3OH (blue line) and after the addition of 200µl of TFA to the same solution (red line).

2.3.1 Ground State Properties

Due to the presence of several rapidly exchanging tautomers and conformers in solution, different structures of **PCCox** have been fully optimized in our work in order to identify the most stable conformation. Actually, the increase of the size of the macrocycle from porphyrins to expanded ones provides more conformational flexibility which depends on many factors such as the number of pyrrole units, the bridges, the β- or meso-substituents, the possible coordinated metals, the availability of hydrogen bonding interactions, and the degree of protonation.

In a previous theoretical investigation [36], the conformational preferences of [22]- and [24]-pentaphyrins and of their meso substituted derivatives, were investigated in detail using DFT calculations showing as these macrocycles can adopt a variety of intriguing structures which can be interconverted under certain conditions. [36], Actually, pentaphyrins [1.1.1.1.1], which bear five pyrroles regularly connected through meso-carbons, should contain structural frustration because of the addition of a pyrrole and a meso-carbon to the planar porphyrin skeleton. Due to a

severe steric congestion, conformations with inverted pyrroles to achieve a substantial steric relief and favorable intramolecular hydrogen bonding interactions, have been previously reported. [37-40]

On the basis of such indications, the conformational preferences of the title molecule **4** have been investigated using density functional calculations. The explored structures are reported in Figure 3 and the main geometrical parameters are collected in Table S1 of the Supplementary Material.

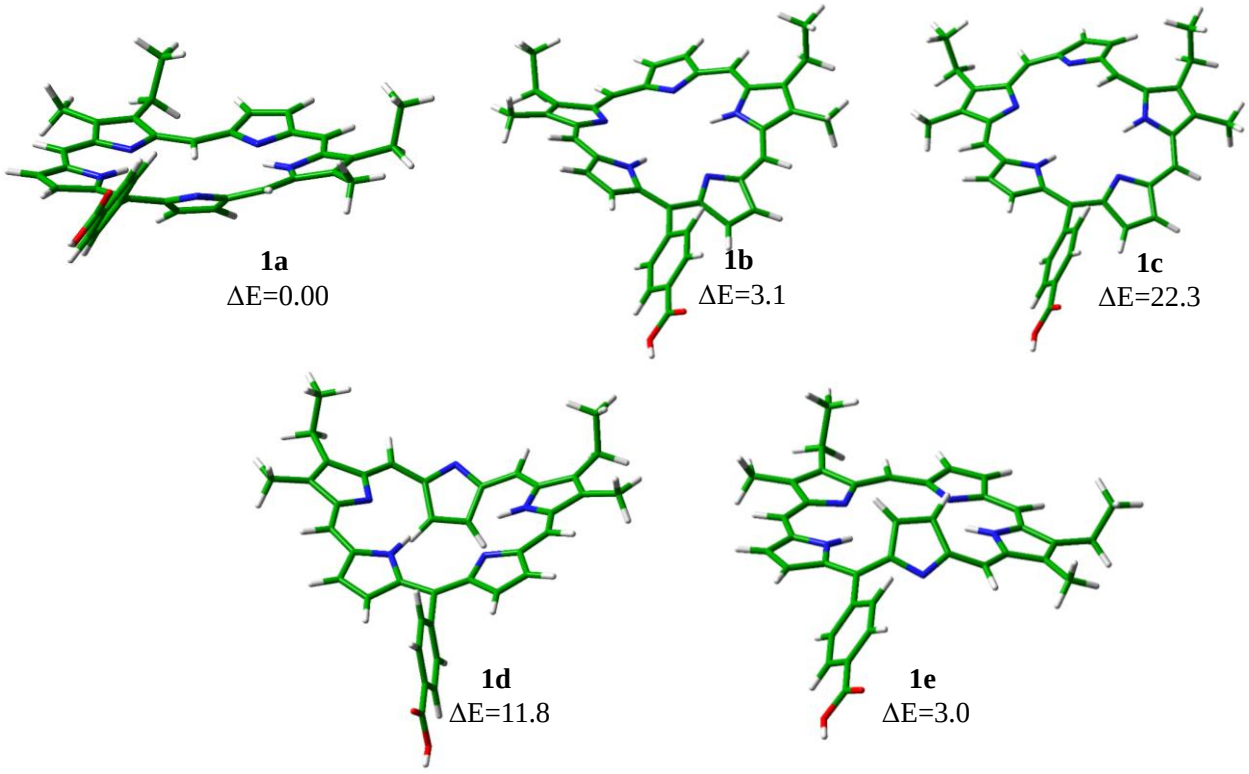

Figure 3. Structures and relative energies of the **PCCox** conformers. Relative energies are given in kcal/mol.

All the conformers are distorted from planarity and lie in an energy range of 22 kcal/mol. The most stable conformer, named **1a**, has four inward-pointing pyrroles with a meso-proton flipped inside the ring and one outward-pointing pyrrole. The inverted pyrrolic ring thus, points its nitrogen out of the porphirinoid cavity (φ8= -156°), and this structure is reminiscent of the

similar conformation of 5,10,15,20-tetraphenylsapphyrin [37-39] and of 5,10,20,25-tetrakis(pentafluorophenyl) substituted hexaphyrin. [40] Compared to the other conformer, the resulting two intramolecular hydrogen bonds appear stronger owing to the shorter NH-N distances, contributing such interactions, to the stabilization of the structure. (Table S1)

The same pyrrolic ring (*E*) is inverted also in the **1e** isomer, but in that conformer, the proton of the meso-carbon between pyrroles *B* and *C* points out of the cavity. The less favorable intramolecular H-bonding interactions with respect to **1a**, leads to a slight destabilization of the energy of about 3 kcal/mol.

In the **1b** structure, which is isoenergetic with the **1e**, all the subunits have a cic-cis alignment so all the nitrogen atoms point inward. The resulting geometry is just slightly distorted from the planarity. On the contrary, the relative stabilities of the conformations **1c** and **1d** are energetically far from the most stable one.

Benchmark of XC Functionals and Electronic Absorption Spectra

The presence in solution of different conformers makes complicated the interpretation of the experimentally recorded UV-Vis spectra (Figure 2), since the assignment of the transitions just to one conformer could be misleading. Therefore, to better characterize the spectral features of molecule **4**, the UV-Vis spectrum of each **PCCox** conformer has been computed at TDDFT level of theory, also taking into account several protonation states of the most stable ones.

In order to select the most appropriate XC functional to accurately describe the electronic transition energies for the systems under evaluation, a series of preliminary computations have been carried out testing different XC density functionals against the experimental spectrum reported in Fig. 2. In particular, B3LYP, cam-B3LYP, PBE0, ωB97XD, M06 and M06L have been employed to obtain the electronic absorption spectra of the conformers 1a-1e. B3LYP, M06

and PBE0 give similar results predicting the same trends for all the investigated conformers. By employing ωB97XD and cam-B3LYP functional, a similar band shape systematically translated toward lower wavelength is obtained for each compound. On the contrary, the local functional M06-L gives unique results, which are not easily comparable to those of the other functionals. The UV-Vis spectra obtained by using the above mentioned XC-functionals are reported in the Supplementary Material.

M06 has proven to better reproduce the maximum absorption peak in the Q-band and it has been chosen as the most suitable XC functional for the description of all the other considered systems. This result also agrees with other previous benchmarks confirming that the use of 20-30 % of HF exchange provides, in most cases, accurate results. [41,42]

The M06/6-31+G* excitation energies in methanol solvent for the low lying conformers of **PCCox** are reported in Table 1. UV-Vis spectra for each conformer and overposition of them is reported in Figure 4.

Table 1. Main vertical singlet electronic energies ΔE (eV, nm), oscillator strengths f and main configuration (with contribution in %) for the different conformations of **PCCox**, in methanol solvent at M06/6-31+G* level of theory.

ΔE (eV, nm) M06	Main Configuration (%)	f
	PCCox (**1a**)	
1.65, 751	H→L (69)	0.042
2.55, 486	H→L+1 (55); H-1→L (40)	1.022
2.63, 472	H-1→L (57)	1.145
	PCCox (**1e**)	
1.69, 735	H→L (60)	0.017
1.80, 688	H→L+1 (52); H-1→L (48)	0.017
2.55, 486	H-1→L (30); H→L+1 (29);H-1→L+1 (21)	1.553
2.62, 474	H-1→L+1 (35); H→L (22); H→L+1 (20)	1.271
	PCCox (**1b**)	
2.70, 459	H-2→L (26); H→L+1 (18);H-1→L (18)	1.160
2.76, 450	H-1→L (34); H→L (27)	1.614

2.87, 433	H-2→L (64); H→L+1 (14)	0.902
	PCCox (**1d**)	
2.61, 475	H→L+1 (30); H-1→L (22); H-1→L+1 (17)	0.988
2.66, 466	H-1→L+1 (37); H→L (24); H→L+1 (13)	1.253
2.85, 435	H-2→L (74%)	0.531
	PCCox (**1c**)	
2.57, 481	H-2→L+1 (35); H-1→L (18); H-2→L (18)	0.961
2.65, 468	H-2→L (22); H→L+1 (24); H-2→L+1 (22)	1.337
2.88, 430	H-3→L (58)	0.362
exp **462, 792**		

The experimental intense Soret band at 462 nm is well reproduced by all the conformers considered in our investigation. Two or more Q-bands have been theoretically characterized for each structure. Nevertheless, only two conformers show absorption band in the red region of the spectrum. Indeed, compound **1a** show one weak transition at 751 nm that is mainly HOMO→LUMO (69%) in nature. The most intense transition energy is the Soret band, which is composed by two transition configurations of almost equal weight found at 486 nm and 472 nm. As evidenced in Table 1, these peaks are due to a HOMO→LUMO+1 (55%) and to a HOMO-1→LUMO (57%) transitions, respectively.

The experimental Soret band at 462 nm is well reproduced also by conformer **1e**, whose spectra is characterized by two strong transitions computed at 486 nm and 474 nm. Moreover, two very weak transitions are found also at higher wavelength, computed at 735 nm and 688 nm.

On the contrary, conformers with no inverted pyrrolic ring (**1b**, **1c** and **1d**) don't show any transition in the red part of the spectrum. Such results allow us to shed light on the conformational preferences of pentaphyrin **4**. Although the unequivocal ascription of the experimental spectrum of free **PCCox** to just one conformer could be misleading, our data clearly suggest the presence, in neutral solution, of conformers with inverted pyrroles (**1a** and

1e). It's noteworthy that, from energetic point of view, such conformations are the preferred ones in neutral conditions, while at least two of the five hypothesized conformers (**1c** and **1d**) can be ruled out.

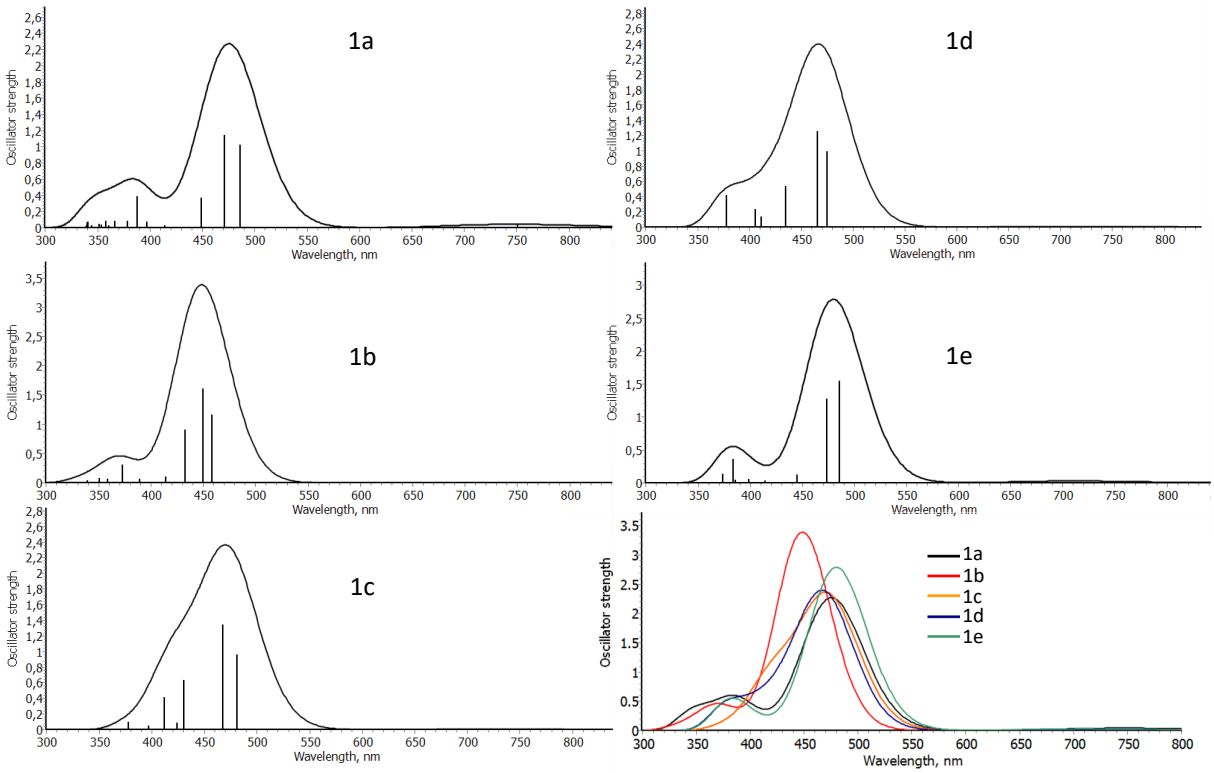

Figure 4. Computed absorption spectra for the 1a-1e conformations of **PCCox**, in methanol solvent at M06/6-31+G* level of theory.

In acid conditions, besides the Soret band red-shifted at 480 nm and the appearance of a second peak at 508 nm, the UV-Vis spectra shows another band located at 617 nm. No changes are observed in the NIR region, being the band centered at 792 nm as in neutral conditions (Figure 2). TFA is likely to promote the formation of positively charged species of **PCCox**. As a consequence, the absorption spectra of protonated **1a, 1e** and that obtained for structure **1b,** have been computed and the results are shown in Table 2. From energetic point of view, the increasing of acidic conditions favours conformation with meso protons flipped outside the cavity,

becoming **1e** and **1b** the preferred conformations in their highly protonated states, while **1a** conformation is the most stable one in neutral and mono-protonated state.

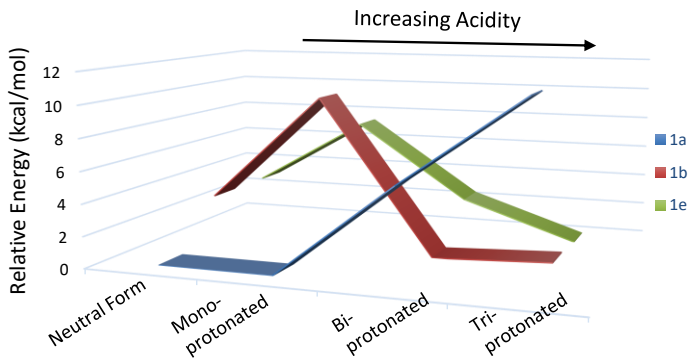

Figure 5. Variation of the relative stabilities of conformers 1a, 1b and 1e with the increasing of acidity.

The computed UV-Vis spectra in acid conditions, confirm a slight shift of the Soret band toward higher wavelengths in the case of highly protonated form of isomer **1b.** Surprisingly, in its fully protonated form, conformer **1b** show transitions in the red part of the spectrum (731 nm and 720 nm), missing in the computed spectra of the neutral counterpart. It is worth of note that in the experimental conditions (CDCl3 containing 33% of TFA), **PCCox** is supposed to be fully protonated. Our data suggest that acid conditions promotes the formation of conformer having a cis-cis alignment of the subunits, i.e. with all the pyrroles pointing inward, confirming the experimental observations. Indeed, no significant changes in the spectra of fully protonated **1a** and **1e** conformers are registered, compared to those computed in neutral conditions.

Moreover, this evidence is in accordance with the above mentioned relative stabilities of the conformers in solutions, which suggests that isomer **1b** becomes more abundant with the increasing of acidity (Figure 5). Additionally, the computed ^{1}H-NMR chemical shifts are also

consistent with the presence of fully protonated **1b** conformer in solution. (See Table 3 of Supplementary Material).

Nevertheless, the experimental bands found at 508 and 617 nm cannot be assigned to any fully protonated conformers (Figure 2). Actually, on the basis of our computations, a transition at 500 nm characterizes the spectrum of mono-and bi-protonated **1a** species and is found also in the spectrum of monopratonated **1e** conformer. The very weak band at 617 nm can be assigned only to **1e** conformer, in its mono and bi-protonated form.

Table 2. Main vertical singlet electronic energies ΔE (nm), oscillator strengths f and main configuration (with contribution in %) for different protonation state of **PCCox** (**conformers 1a,1b and 1e**), in methanol solvent at M06/6-31+G* level of theory.

ΔE/ nm	**Main Configuration (%)**	**f**	**ΔE/ nm**	**Main Configuration (%)**	**f**	**ΔE/ nm**	**Main Configuration (%)**	**f**
	$1a^{+}$			**$1b^{+}$**			**$1e^{+}$**	
743	H→L(68)	0.052	462	H→L+1 (34); H-1→L (30)	1.120	726	H→L (62)	0.040
500	H-2→L (42); H-1→L (22)	0.581	456	H-2→L+1 (44)	0.886	694	H-1→L (52)	0.005
489	H-2→L (35); H-1→L (32)	0.603	450	H-2→L+1 (37)	1.336	500	H-2→L (83)	0.135
464	H-1→L+1 (45)	1.390				477	H→L+1 (46)	1.343
	$1a^{+2}$			**$1b^{+2}$**			**$1e^{+2}$**	
728	H→L(47)	0.039	471	H-1→L+1 (50)	1.201	728	H→L(56)	0.030
500	H→L+1 (37): H-1→L (30)	0.710	469	H-1→L (50); H→L+1 (50)	2.162	696	H→L+1 (58)	0.043
473	H-2→L+1 (45)	0.795				477	H-1→L (52)	1.628
459	H-1→L+1 (42)	1.533				473	H-1→L+1 (54)	1.451
	$1a^{+3}$			**$1b^{+3}$**			**$1e^{+3}$**	
724	H→L(60)	0.026	731	H→L (61)	0.025	732	H→L (65)	0.049
478	H→L+1 (51)	1.148	720	H→L +1 (54)	0.029	711	H→L +1 (57)	0.065
461	H-1→L+1 (45)	1.567	474	H-1→L (50)	2.294	484	H-1→L (52)	1.935
			471	H-2→L+1 (58)	1.385	472	H-1→L+1 (60)	1.379
	exp	**462, 792** in MeOH **480, 508 627, 792** in MeOH + 200μl TFA						

2.3.2. Type II photoreactions

From a photophysical point of view, a clinically successful sensitizer agent able to generate a type II photochemical reaction must have a singlet-triplet energy gap higher than that required to excite the molecular oxygen from its triplet ground state to the singlet one (0.98 eV). Actually, it is well known that $^1O_2$ represent the cytotoxic agent in the type II PDT reactions since it can react with several biological molecules, including lipids, proteins, and nucleic acids, leading to cancer cell death.

$Ps(T_1) + {}^3O_2 \rightarrow Ps(S_0) + {}^1O_2$

In order to verify if such process occurs, the gap between the singlet ground state and the first triplet excited one has been computed for **PCCox**. Results (see Table 1) show that for **PCCox 4** the $\Delta E_{S\text{-}T}$ is 1.15 eV that results to be 0.17 eV higher than that required to promote the $^3\Sigma g^- \rightarrow {}^1\Delta g$ electronic transition for molecular oxygen. This means that **PCCox 4** is able to produce the cytotoxic agent. The comparison between the $\Delta E_{S\text{-}T}$ herein computed for **4** and that previously found for the reduced species **3** [25] (< 0.2 eV) can explain the observed differences between these two expanded porphyrins. [24] Actually, in view of the very small energy $\Delta E_{S\text{-}T}$ gap found for the isopentaphirin, the ability to generate singlet oxygen by means of a type II PDT mechanism was ruled out. [25]

Table 3. First Excited state energy (E_{ex}), Ground State Vertical Electron Affinities (VEA), and Ionization Potentials (VIP) for O_2 and PCCox in eV, calculated at the B3LYP/6-31+G* level, in water (methanol).

	E_{ex}	VEA	VEA (T1) [a]	VIP	VIP (T1) [b]
PCCox	**1.15**	**-3.46 (-3.54)**	**-4.61 (-4.69)**	**5.19 (5.13)**	**4.04 (3.98)**
O_2	**0.90**	**-3.20 (-3.14)**		**9.86 (9.92)**	

[a]VEA(T1) = VEA(S0) - E_{ex}
[a]VIP(T1) = VIP(S0) - E_{ex}

2.3.3. VEA and VIP and evaluation of Type I Reaction

As previously mentioned, the PDT activity of a photosensitizer can occur throughout the so-called Type I mechanism. This kind of reaction involves electron or hydrogen-atom transfer between the excited sensitizer (usually T_1) and substrate molecules, such as the cell membrane, to yield radical ions and free radicals. These radicals interact with oxygen to produce oxygenated products. Different pathways can be followed to generate $O_2^{\cdot -}$ species, which can generate other highly reactive radicals (e.g. hydroxyl) that promote reactions with biomolecules. [12]

i) The superoxide anion $O_2^{\cdot(-)}$ can be produced by direct electron transfer from the photosensitizer to molecular oxygen:

$$Ps\ (S_0) + {}^3O_2 \rightarrow Ps^{\cdot(+)} + O_2^{\cdot(-)} \qquad (1)$$

In this case, the reaction occurs if the following condition is satisfied:

$$VEA\ ({}^3O_2) + VIP\ (Ps(S_0/T_1)) < 0$$

ii) The second pathway to generate $O_2^{\cdot(-)}$ may proceed through electron transfer from the reduced form of PS to molecular oxygen

$$Ps^{\cdot(-)} + {}^3O_2 \rightarrow {}^1Ps + O_2^{\cdot(-)} \qquad (2)$$

This reaction is possible only if the summation of the electron affinity of ${}^3O_2$ and VEA PS (S_0/T_1) is negative: $VEA({}^3O_2) - VEA\ Ps\ (S_0) < 0$.

The $Ps^{\cdot(-)}$ species could be formed in solution through the so-called autoionization reactions which represent the precondition of reaction (2) and imply the reduction of T_1 state of Ps by neighboring S_0 or T_1 state of Ps itself. (Eqs. (3) and (4))

$$Ps\ (T_1) + Ps(S_0) \rightarrow Ps^{\cdot +} + Ps^{\cdot -} \qquad (3)$$

$$Ps\ (T_1) + Ps(T_1) \rightarrow Ps^{\cdot +} + Ps^{\cdot -} \qquad (4)$$

Such reactions take place if the summation of VEA (T1) with VIP (S0) or VIP (T1) is negative:

$VEA(T_1) + VIP(S_0) < 0$
$VEA(T_1) + VIP(T_1) < 0$

In order to verify if the considered systems are able to promote these reactions, we have computed vertical electron affinities and ionization potential for **PCCox,** in both water and methanol solvent (see Table 1).

On the basis of the reported values, the reactions (1), (2) and (3) cannot occurs. Only reaction (4) takes place since the summation of VEA (T_1) and VIP (T_1) is negative, meaning that $PCCox^{\cdot-}$ can be formed but it seems not able to pass one electron to $^3O_2$ to form $O_2^{\cdot-}$ (Eq. (2)) theoretically judging from the positive total reaction energy (+0.26 and 0.4 eV, in water and methanol, respectively).

Conclusions

A joint experimental and theoretical investigation on oxidized [1.1.1.1.1] pentaphyrin has been herein presented. The following conclusions can be drawn:

- 22π-electrons [1.1.1.1.1] pentaphyrin **4** has been successfully prepared and fully characterized by NMR, UV-Vis, mass spectra and theoretical calculations.
- Due to the presence of several rapidly exchanging tautomers in solution, the conformational preferences of pentaphirin **4** were investigated exploring different conformers of title compound, by means of DFT calculations.

- The experimental UV-Vis transitions have been fully assigned and interpreted. The computed absorption spectra allowed us to propose the presence, in neutral solution, of conformers with inverted pyrroles (**1a** and **1e**).
- On the contrary, our computations suggest that acid conditions favors fully protonated conformers having a cis-cis alignment of the subunits (i.e. **1b**). Nevertheless, pentaphyrins having inverted pyrroles in their mono- and bi-protonated forms can co-exist in solutions.
- Computed VEA and VIP values reveal that these compounds are not able to generate superoxide anion $O_2^{\cdot(-)}$ and then type-I photoreactions cannot occur.
- From the computed energy gaps between singlet ground and low lying triplet excited state emerges that the systems are able to produce the cytotoxic agent $^1O_2$ (Type II reactions) which could act as a primary oxidant in the photosensitized transformation of organic substances, supporting the use of the tested compound in environmental application for water treatment and photo-disinfection processes.

Experimental and computational details

Chemistry. All solvents and chemicals were of reagent grade quality and were used as received from the suppliers. Mass spectra were recorded on a ion trap Finnigan Mat GCQ (Finnigan MAT, Austin, Texas, USA), operated in electron ionization mode, and on a Finnigan LXQ linear ion trap Mass Spectrometer (Thermo Scientific, Waltham, MA, USA) equipped with a ESI source. Experiments were carried out in the positive ion mode. EI mass spectrums were performed on a Micromass VG 7070 H mass spectrometer operating at 70 eV (Micromass Ltd., Manchester, UK). ^{1}H NMR spectra were recorded on a Bruker AM-200 (200 MHz). Chemical

shifts are given in ppm (δ) relative to tetramethylsilane (^{1}H NMR) as an internal standard or to the peak of the solvent used (^{13}C NMR). 2D NMR experiments (COSY and NOESY) were performed using the standard pulse sequences from the Bruker library. UV-Vis spectra were measured on a Varian Cary 50 (Palo Alto, CA, USA) spectrophotometer using 1.0 cm quartz cuvettes.

PCCox 4. (20-[4'-(carboxy)]phenyl-2,13-dimethyl-3,12-diethyl-[22]pentaphyrin) 50 mg (0.072 mmol) of 3 [4c] was dissolved in a mixture of CH_2Cl_2/TFA 1 : 1 (5 mL), and stirred for 48 h in the air at room temperature. The dark solution was washed with 10% NaOH solution (3 x 5 mL), and then with distilled water (2 x 5 mL). The crude product, obtained after evaporation of the solvent, was purified by HPLC. The oxidation of 3 to 4 was quantitative. 1H NMR (200 MHz, $CDCl_3$ 33% TFA, 20 °C, TMS): δ = 12.85 (s, 2H, meso-C*H*), 12.77 (s, 2H, meso-C*H*), 11.37 (s, 2H, H pyrrole), 10.75 (d, 2H, H pyrrole), 10.00 (d, 2H, H pyrrole), 8.12 (d, 2H, H phenyl), 7.43 (d, 2H, H phenyl), 4.99 (q, 4H, C*H*$_2$CH$_3$), 4.5 (s, 6H, CH$_3$), 2.35 (t, 6H, CH$_2$C*H*$_3$), -4.73 (br s, 2H, NH), -4.93 (br s, 1H, NH), -5.07 ppm (br s, 2H, NH); UV-vis (TFA) λ_{max} (nm): 460 (log ε = 5.13), 647 (log ε = 3.96), 797 (log ε = 3.58); MS (ESI, positive mode, AcN): *m/z* 592 ($[MH]^+$), 610 ($[MH + H_2O]^+$)).

Computational details. All the calculations herein presented have been performed at DFT and its time-dependent TD-DFT formulation [28] by using Gaussian 09 program code.[43] Geometry optimization have been performed without constrains by using the B3LYP exchange-correlation functional in conjunction with 6-31+G* basis sets [44-45]. Vibrational frequencies, computed with the same level of theory, have been used in order to verify the minimum nature of the optimized structures.

Electronic absorption spectra have been calculated in solvent testing different XC density functionals against the experimental spectrum (B3LYP, cam-B3LYP, PBE0, ωB97XD, M06 and M06L). M06 has proven to better reproduce the maximum absorption peak in the Q-band and it has been chosen as the most suitable XC functional for the description of the considered systems.

The integral equation formalism polarizable continuum model (IEFPCM) [46-48], which corresponds to a linear response in non-equilibrium solvation, has been employed to reproduce the bulk solvent effects. The dielectric constants of methanol ($\varepsilon = 32.61$) has been set up along with the default cavity generation parameters.

The vertical triplet energies for PCCox has been obtained over the ground state (S0) electronic configuration in water, at B3LYP/6-31+G* level of theory. The triplet–singlet energy gap of O_2 has been evaluated at the same level of theory, adopting the method proposed by Ovchinnikov and Labanowski [49] to correct the contaminated energy of the singlet state. Following that procedure, a singlet state corrected energy and a triplet–singlet energy gap of 0.90 eV were obtained, in very good agreement with the experimental value.

NMR calculations were carried out using the GIAO formalism [50], at B3LYP/IGLO-III level of theory, in chloroform solvent. This protocol has been previously suggested as particularly accurate for the computation of magnetic properties of organic molecules [51-52]. Nevertheless, cam-B3LYP, PBE0, ωB97XD, M06 and M06L XC functional have been also tested and no significant differences among the obtained chemical shifts have been observed. The results are reported in the Supplementary Material.

ASSOCIATED CONTENT

Supplementary Material. ESI-MS of PCCox, computed main Bond lengths (Å) and main dihedral angles (degrees) for PCCox, main vertical singlet electronic energies for several conformations of PCCox obtained with different XC functionals in methanol, computed UV-Vis Spectra, NMR computations.

AUTHOR INFORMATION

Corresponding Author

*To whom correspondence should be addressed:

E-mail: marta.alberto@chimie-paristech.fr ; tel. +33 (0)1 44 27 66 72; Fax: +33 (0)1 43 29 20 59

ACKNOWLEDGMENT

M.E.A. would like to thank the Research Executive Agency (REA) and European Commission for the MSCA Individual Fellowship grant (call: H2020-MSCA-IF-2014, Project ID: 652999). This work was granted access to the HPC resources of MesoPSL financed by the Region Ile de France and the project Equip@Meso (reference ANR-10-EQPX-29-01) of the programme Investissements d'Avenir supervised by the Agence Nationale pour la Recherche. Università della Calabria, Università di Udine and ENSCP are gratefully acknowledged.

BIBLIOGRAPHY

[1] Stepien M, Sprutta N, Latos-Grazynski L, (2011) Angew Chem Int Ed, 50:4288-4340

[2] Osuka A, Saito S (2011) Angew. Chem. Int. Ed. 50:4342-4373

[3] Qian G, Wang ZY (2010) Chem Asian J 5:1006-1029

[4] Sessler JL, Davis JM (2001) Acc Chem Res 34:989-997

[5] Ikawa Y, Takeda M, Suzuki M, Osuka A, Furuta H (2010) Chem Comm 46:5689-5691

[6] Tanaka T, Aratani N, Lim JM, Kim KS, Kim D, Osuka A (2011) Chem Sci 2:1414-1418

[7] Sarma T, Panda PK (2011) Chem Eur J 17:13987-13991

[8] Sessler JL, Seidel D (2003) Angew Chem Int Ed 42:5134-5175

[9] Jasat A, Dolphin D (1997) Chem ReV 97:2267-2340

[10] Lang K, Monsinger J, Wagnerova DM (2004) Coord Chem ReV 248:321-350

[11] DeRosa MC, Crutchley RJ (2002) Coord Chem Rev 233-234:351-371

[12] Yano S, Hirohara S, Obata M, Hagiya Y, Ogura S, Ikeda I, Kataoka H, Tanaka M, Joh T (2011) J Photochem Photobiol C 12:46-67;

[13] Allison RR, Bagnato VS, Sibata CH (2010) Future Oncol 6:929-940

[14] MacDonald IJ, Dougherty TJ (2001) J Porphyr Phthalocya 5:105-129;

[15] Dolmans DE, Fukumura D, Jain RK (2003) Nat Rev Cancer 3:380-387

[16] Kim H, Kim W, Mackeyev Y, Lee G-S, Kim H-J, Tachikawa T, Hong S, Lee S, Kim J, Wilson LJ, Majima T, Alvarez PJJ, Choi W, Lee J, (2012) Environ Sci Technol 46:9606-9613;

[17] Han SK, Sik RH, Motten AG, Chignell CF, Bilski PJ (2009) Photochem. Photobiol. 85:1299-1305

[18] Kohn T, Nelson KL (2007) Environ Sci Technol 41:192-197

[19] Romero OC, Straub AP, Kohn T, Nguyen TH (2011) Environ. Sci. Technol. 45:10385-10393

[20] Christoforidis KC, Louloudi M, Deligiannakis Y (2010) Appl. Catal. B. Environ. 95:297-302

[21] Gmurek M, Kubat P, Mosinger J, Miller JS (2011) Photochem. Photobiol. A Chem.223:50-56

[22] Comuzzi C, Cogoi S, Overhand M, Van der Marel GA, Overkleeft HS, Xodo LE (2006) J Med Chem 49:196-204

[23] Comuzzi C, Cogoi S, Xodo LE, (2006) Tetrahedron 62:8147-8151

[24] Ballico M, Rapozzi V, Xodo LE, Comuzzi C (2011) Eur J Med Chem 46: 712-720

[25] Fortes Ramos Sousa F, Quartarolo AD, Sicilia E, Russo N (2012) J Phys Chem B 116:10816-10823

[26] Rossi G, Goi D, Comuzzi C (2012) J Water Health 10:390-399

[27] Fedele R, Comuzzi C, Rossi G, Goi D, (2015) US Patent 8940775 B2

[28] Casida ME In Recent Developments and Applications in Density-Functional Theory; J. M. Seminario, Eds.; Elsevier: Amsterdam, The Netherlands, 1996; pp 155-192.

[29] Adamo C, Jacquemin D (2013) Chem Soc Rev 42: 845–856

[30] Alberto ME, De Simone BC, Mazzone G, Quartarolo A D, Russo N (2014) J Chem Theory Comput 10:4006-4013

[31] Alberto ME, Iuga C, Quartarolo AD, Russo N (2013) J Chem Inf Model 53: 2334-2340

[32] Alberto ME, De Simone BC, Mazzone G, Marino T, Russo N (2015) Dyes and Pigments 2015, 120, 335-339.

[33] Alberto ME, Mazzone G, Quartarolo AD, Fortes Ramos Sousa F, Sicilia E, Russo N (2014) J Comput Chem 35:2107–2113

[34] Alberto ME, Marino T, Quartarolo AD, Russo N (2013) Phys Chem Chem Phys 15:16167-16171;

[35] Jacquemin D, Perpete EA, Ciofini I, Adamo C (2009) Acc Chem Res 42: 326–334.

[36] Alonso M, Geerlings P, De Proft F (2013) J Org Chem 78:4419-4431

[37] Rachlewicz K, Sprutta N, Latos-Grazynski L, Chmielewski PJ, Szterenberg L (1998) *J Chem Soc Perkin Trans 2* 959-968

[38] Rachlewicz K, Latos-Grazynski L, Gebauer A, Vivian A, Sessler JL (1999) *J Chem Soc Perkin Trans 2:* 2189-2195

[39] Chmielewski PJ, Latos-Grazyński L, Rachlewicz K (1995) *Chem Eur J 1:* 68-73

[40] Yoneda T, Mori H, Sun Lee B, Yoon M-C, Kim D, Osuka A (2012) *Chem Commun 48:* 6785-6787

[41] Latouche C, Skouteris D, Palazzetti F, Barone V (2015) J *Chem Theory Comput* 11: 3281–3289

[42] Holland JP, Green JC (2010) *J Comput Chem 31:*1008–1014.

[43] Gaussian 09, Revision D.01, Frisch, M. J.; Trucks, G. W.; Schlegel, H. B.; Scuseria, G. E.; Robb, M. A.; Cheeseman, J. R.; Scalmani, G.; Barone, V.; Mennucci, B.; Petersson, G. A.; Nakatsuji, H.; Caricato, M.; Li, X.; Hratchian, H. P.; Izmaylov, A. F.; Bloino, J.; Zheng, G.; Sonnenberg, J. L.; Hada, M.; Ehara, M.; Toyota, K.; Fukuda, R.; Hasegawa, J.; Ishida, M.; Nakajima, T.; Honda, Y.; Kitao, O.; Nakai, H.; Vreven, T.; Montgomery, J. A., Jr.; Peralta, J. E.; Ogliaro, F.; Bearpark, M.; Heyd, J. J.; Brothers, E.; Kudin, K. N.; Staroverov, V. N.; Kobayashi, R.; Normand, J.; Raghavachari, K.; Rendell, A.; Burant, J. C.; Iyengar, S. S.; Tomasi, J.; Cossi, M.; Rega, N.; Millam, J. M.; Klene, M.; Knox, J. E.; Cross, J. B.; Bakken, V.; Adamo, C.; Jaramillo, J.; Gomperts, R.; Stratmann, R. E.; Yazyev, O.; Austin, A. J.; Cammi, R.; Pomelli, C.; Ochterski, J. W.; Martin, R. L.; Morokuma, K.; Zakrzewski, V. G.; Voth, G. A.; Salvador, P.; Dannenberg, J. J.; Dapprich, S.; Daniels, A. D.; Farkas, Ö.; Foresman, J. B.; Ortiz, J. V.; Cioslowski, J.; Fox, D. J. Gaussian, Inc., Wallingford CT, 2009.

[44] Ditchfield R, Hehre WJ, Pople JAJ (1971) Chem Phys 54:724-728;

[45] Hehre WJ, Ditchfield R, Pople JAJ (1972) Chem Phys 56:2257-2261;

[46] Cossi M, Barone V, Mennucci B, Tomasi J (1998) Chem Phys Lett 286:253-260

[47] Cossi M, Scalmani G, Rega N, Barone V (2002) J. Chem Phys 117:43-54

[48] Tomasi J, Mennucci B, Cammi R (2005) Chem Rev, 105:2999–3094.

[49] Ovchinnikov AA, Labanowski JK (1996) Phys. Rev. A, 56:3946–3952.

[50] Becke AD (1993) J. Chem. Phys., 98:1372-1377

[51] Magyarfalvi G, Pulay P. (2003) J. Chem. Phys. 119:1350-1357

[52] Di Tommaso S, David P, Picolet K, Gabant M, David H, Morançais J-L, Gomar J, Leroy F, Adamo C (2013) 3:13764-13771

Table of Contents Graphic and Synopsis

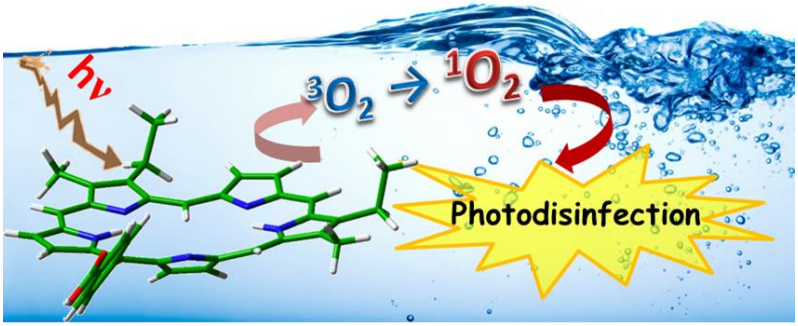

22π-electrons [1.1.1.1.1] pentaphyrin as a new photosensitizing agent for water disinfection: Experimental and Theoretical characterization